

# 8 The $\pi^+ \rightarrow e^+ \nu_e / \pi^+ \rightarrow \mu^+ \nu_\mu$ branching ratio

P. Robmann, A. van der Schaaf and P. Truöl

in collaboration with University of Virginia, Charlottesville, USA; Institute for Nuclear Studies, Swierk, Poland; JINR, Dubna, Russia; PSI, Villigen, Switzerland and Rudjer Bošković Institute, Zagreb, Croatia

(PEN Collaboration)

Within the Standard Model, assuming  $V - A$  structure of the electroweak interaction, pion decays are helicity-suppressed ( $l$  stands for  $e$  and  $\mu$ ):

$$\Gamma[\pi^+ \rightarrow l^+ \nu_l(\gamma)] = \frac{G_\mu^2 |V_{ud}|^2}{4\pi} F_\pi^2 m_\pi m_l^2 \left[1 - \frac{m_l^2}{m_\pi^2}\right] + h.c.,$$

where  $G_\mu$  indicates that the Fermi coupling constant is taken from the muon lifetime. The largest uncertainty comes from the pion decay constant  $F_\pi$  which accounts for the non-perturbative strong interactions between the quarks inside the pion. In fact, the measured pion decay time  $\tau_\pi = 26.033(5)$  ns is used to measure  $F_\pi$  which is an important parameter in strong-interaction physics.

28 Most theoretical (and experimental!) uncertainties cancel when studying the branching ratio

$$B \equiv \Gamma[\pi^+ \rightarrow e^+ \nu_e(\gamma)] / \Gamma[\pi^+ \rightarrow \mu^+ \nu_\mu(\gamma)].$$

The Standard Model value of the  $\pi^+ \rightarrow e^+ \nu_e / \pi^+ \rightarrow \mu^+ \nu_\mu$  branching ratio, calculated assuming  $V - A$  and a universal  $Wl_i \nu_i$  coupling strength, is  $1.2353(1) \times 10^{-4}$  [1]. A measurement of the branching ratio would allow sensitive tests of these two fundamental ingredients of the Standard Model. The present experimental result  $1.2312(37) \times 10^{-4}$  dates back over thirty years [2] and two new experiments [3] aim at a reduction of the error by almost an order of magnitude. A first result of our PIENU friends,  $1.2344 \pm 0.0023(\text{stat}) \pm 0.0019(\text{syst}) \times 10^{-4}$  based on 10% of their data set, was published last year [4].

- [1] V. Cirigliano and I. Rosell, JHEP **10** (2007) 5; Phys. Rev. Lett. **99** (2007) 231801.
- [2] G. Czapek *et al.*, Phys. Rev. Lett. **70** (1993) 17; D. I. Britton *et al.*, Phys. Rev. Lett. **68** (1992) 3000.
- [3] PEN Collaboration, PSI experiment R-05-01 (2005), D. Počanić and A. van der Schaaf, spokespersons; PIENU Collaboration, TRIUMF proposal 1072 (2006), D. Bryman and T. Numaō, spokespersons.
- [4] A. Aguilar-Arevalo *et al.*, [PIENU Collaboration], Phys. Rev. Lett. **115** (2015) 071801.

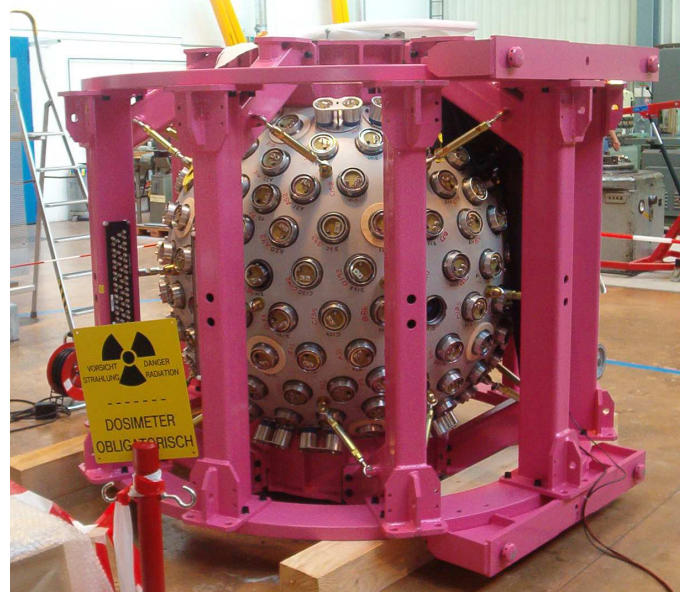


FIG. 8.1 – The PEN pure-CsI calorimeter in the PSI “Montagehalle” before it was mounted on the experimental platform and buried under cabling and thermo-shielding.

## 8.1 PEN data taking

The PEN experiment took data at PSI during the years 2008 - 2010, where the setup varied slightly over the years. The most expensive component by far is a  $3\pi$  Sr spherical pure-CsI calorimeter (see Fig. 8.1) used to measure positron and photon energies. Pure CsI has its main scintillation decay-time component around 28 ns, much shorter than most other organic scintillators.

Pions from the  $\pi$ E1 beam line are brought to rest in a plastic scintillator after having crossed a thin scintillator in an intermediate focus 4 m upstream and a degrader scintillator, situated close to the target scintillator. During 2009/10 a small time-projection chamber (mini TPC) is used to record the trajectories of the incoming pions.

Decay positrons from  $\pi \rightarrow e\nu$  and the sequence  $\pi \rightarrow \mu\nu$ ,  $\mu \rightarrow e\nu\bar{\nu}$ , are tracked in two cylindrical MWPCs. The positron energy is determined primarily with the CsI calorimeter. A cylindrical plastic scintillator hodoscope in front of the calorimeter is used both for timing and for particle identification (in particular to separate decay positrons and protons from pion reactions) through  $\Delta E - E$ .

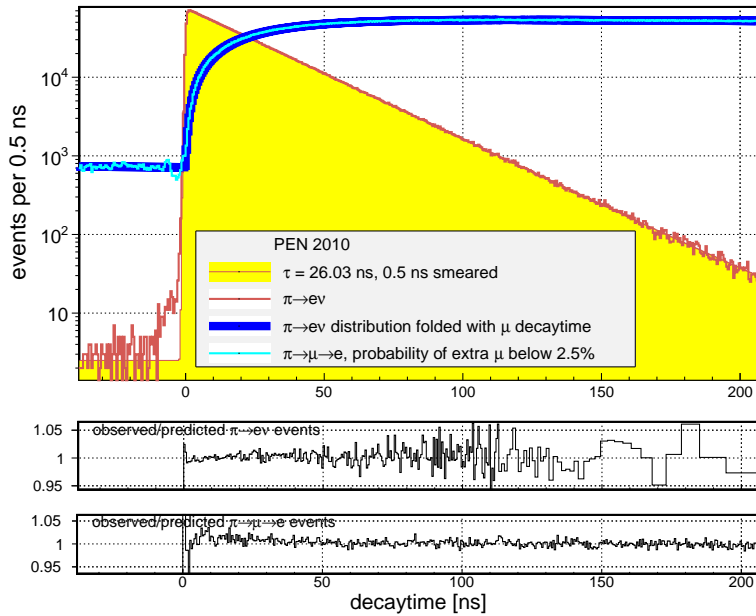


FIG. 8.2 – Observed year 2010  $\pi \rightarrow e\nu$  decaytime distribution. Note the very low background of accidental coincidences and the perfect fit with the expected exponential. Also shown are the prediction for the  $\mu \rightarrow e\nu\bar{\nu}$  branch, obtained by folding with the muon lifetime.

## 8.2 Data analysis and outlook

PEN took data during 2008 - 2010 and has been studying them in great detail ever since. Calibrations are done and most features observed are reproduced by simulation (see previous annual reports for details).

Key observables are the  $e^+$  energy and the  $\pi^+ - e^+$  time delay  $\Delta t_{\pi e}$  (see Figs. 8.2 and 8.3). The decay  $\pi^+ \rightarrow e^+\nu(\gamma)$  peaks at  $0.5 \times m_\pi$  and falls with  $\tau_\pi$ . The decay sequence  $\pi^+ \rightarrow \mu^+\nu$  followed by  $\mu^+ \rightarrow e^+\nu\bar{\nu}(\gamma)$  is characterized by an  $e^+$  energy below  $0.5 \times m_\mu$  and  $\Delta t_{\pi e}$  first rising with  $\tau_\pi$  and then falling with  $\tau_\mu = 2.197 \mu\text{s}$ .

Whereas the  $\pi^+ \rightarrow e^+\nu(\gamma)$  decay was recorded with almost 100% efficiency for  $e^+$  emitted in the calorimeter accep-

tance, the other branch was recorded only for  $\Delta t_{\pi e} < 220$  ns. Events with  $e^+$  energies below  $\approx 48$  MeV were pre-scaled by typically a factor 20.

Systematic uncertainties are associated with the fraction of  $\pi^+ \rightarrow e^+\nu(\gamma)$  events with total energy below  $0.5 \times m_\mu$  and the fraction of  $\pi^+ \rightarrow \mu^+\nu(\gamma)$  decays within the chosen  $\Delta t_{\pi e}$  window. The tail fraction is typically 2% and its value ultimately relies on simulation. The error associated with the time window is minimized by choosing a window corresponding to the situation in which the event rate is equal at both ends. For a 100 ns wide window this happens for 81.4 - 181.4 ns (see Fig. 8.4).

Results for both  $B$  and the structure-dependence of  $\pi \rightarrow e\nu\gamma$  are expected within a year from now.

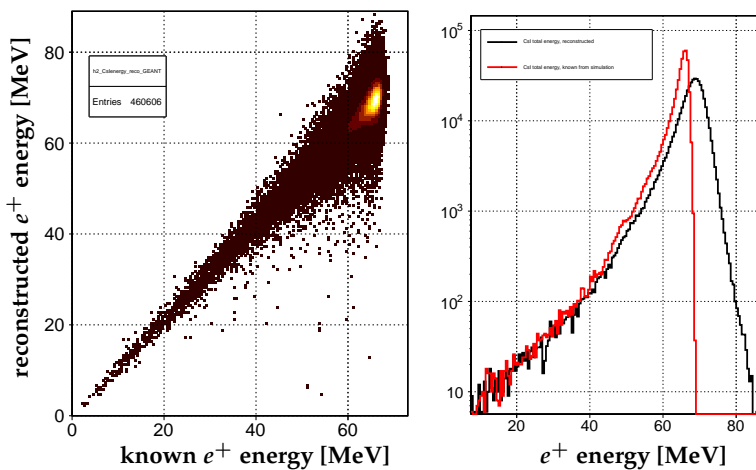


FIG. 8.3 – Scatter plot of reconstructed and known energy deposits from a GEANT  $\pi \rightarrow e\nu$  simulation (left). The right panel shows the two projections. Note the structure, around 50 MeV, for example, which is caused by hadronic interactions followed by neutron escape.

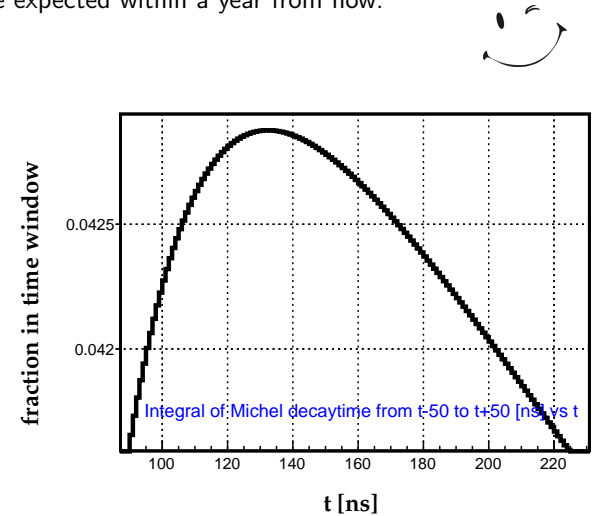


FIG. 8.4 – Fraction of  $\pi \rightarrow \mu \rightarrow e$  events with a  $\pi - e^+$  time delay in a window  $t \pm 50$  ns, versus  $t$ . The distribution peaks at 131.4 ns but falls less than  $10^{-5}$  when moving 1 ns away from that value.